Manuscript prepared for Clim. Past
with version 3.2 of the LaTeX class copernicus.cls.
Date: 20 November 2012

Investigating the past and recent δ^{18}O-accumulation relationship seen in Greenland ice cores

S. L. Buchardt, H. B. Clausen, B. M. Vinther, and D. Dahl-Jensen

Centre for Ice and Climate, NBI, University of Copenhagen, Juliane Maries Vej 30,
2100 Copenhagen OE, Denmark

Correspondence to: S. L. Buchardt (lilja@gfy.ku.dk)

Abstract. Decadal means of δ^{18}O and accumulation rates from 52 ice core sites in Greenland are presented. The accumulation rates are derived from annual layers determined in the δ^{18}O curve. Investigation of the δ^{18}O-accumulation relationship across the ice divide reveals a significant Foehn effect with anticorrelation of δ^{18}O and accumulation rate on the lee side of the divide in Southern Greenland, while no effect is seen in Central Greenland. Furthermore, the sensitivity of accumulation rate to changes in temperature is found to be smaller in Northern Greenland than in the central and southern parts. Four sites in the data set contain sufficient recent data that the period of observed temperature rise from the 1990's and onwards can be investigated. All four sites are located close to the ice divide in Northern Greenland and while three sites show increased temperatures, no conclusive statement can be made about the accumulation rate from these data.

1 Introduction

During the last decades, global temperatures have increased and are affecting global sea level which is currently rising at a rate of $3.11 \pm 0.6\,\mathrm{mm\,yr^{-1}}$ (1993–2008) (Ablain et al., 2009). Continental ice is a significant contributor to this rise in sea level, but the uncertainty on the contribution is not well constrained, as pointed out by the IPCC panel in the AR4 report from 2007 (IPCC, 2007). The Greenland ice sheet constitutes the second largest continental ice mass and holds enough ice to increase global sea level by 7 m if melted completely. Observations have shown that coastal temperatures in Greenland have increased over the last decades (Box, 2002), the area of surface melting is growing (Abdalati and Steffen, 2001) and the ice loss has been estimated to $205 \pm 50\,\mathrm{Gt\,yr^{-1}}$ (2005–2006) (AMAP, 2011). Few measurements exist from the interior part of the ice sheet, but GC-Net automated weather stations have observed rising temperatures (Box et al., 2009). Regional climate model runs indicate that the rise in temperature should be followed by an increase in accumulation rate over the ice sheet, because the warmer air can contain more moisture (Box et al., 2006). Furthermore, several authors have determined empirical relationships between temperature and accumulation rates that also indicate that accumulation should increase with rising temperatures (Dahl-Jensen et al., 1993; Dansgaard et al., 1993; Johnsen et al., 1995). Dahl-Jensen et al. (1993) found the following relation between accumulation rates and δ^{18}O in the GRIP ice core.

$$A = 0.23\exp(0.117(\delta^{18}\mathrm{O} + 34.83)), \tag{1}$$

where A is the ice equivalent accumulation rate in $\mathrm{m\,yr^{-1}}$ and the δ^{18}O values are given in ‰. The factor 0.23 was chosen because the present day mean ice equivalent accumulation rate at GRIP is $0.23\,\mathrm{m\,yr^{-1}}$.

In the following we will first investigate the relationship between temperature and accumulation rate by using δ^{18}O data from Greenland ice cores, and then we will use this as a foundation to look for recent changes in temperature and accumulation rate. Furthermore, we will investigate the geographical differences in the relationship between δ^{18}O and accumulation rate.

2 Data

Accumulation rates and temperatures for 52 sites in Greenland are inferred from ice core δ^{18}O data. The 52 sites and the time period covered at each site are listed in Table 1, and their locations are shown in Fig. 1. Most of the available ice core data are from cores drilled in the 1970's and 1980's and thus do not contain information on the recent period of warming. Therefore, a number of firn cores were drilled and measured for δ^{18}O under the Ice2Sea Programme to either extend existing records to the present or to obtain data from new sites, thus increasing the amount of available data for this period. Where several cores exist from the same site, a composite δ^{18}O record has been created.

3 Method

It has been established that the annual mean δ^{18}O value at a given site on an ice sheet is closely related to the mean annual temperature at that site (Dansgaard, 1953, 1964). Johnsen et al. (1989) found the following empirical relation for sites located on the Greenland ice sheet

$$\delta^{18}\mathrm{O} = 0.67 \times T - 13.7, \tag{2}$$

where T is the temperature in °C and the δ^{18}O is given in ‰. As this relationship is linear, we choose to compare the accumulation rates to δ^{18}O directly instead of to the temperatures calculated from the δ^{18}O.

All timescales used in this study are based on annual layer counting in the δ^{18}O curve (Hammer et al., 1978). This is done by identifying the winter minimum in δ^{18}O for each year and then counting backwards from the surface and down, thus obtaining a chronology for the ice core. If known reference horizons exist for the ice core, e.g. historically dated volcanic eruptions recorded in the electrical conductivity measurement (ECM) record, these can be used to lock the age at these depths. Many other types of ice core data show annual cycles and can be used to identify annual layers. These include chemical components (Legrand and Mayewski, 1997), visual stratigraphy (Alley et al., 1997) and electrical properties (Hammer, 1980). In the present study, δ^{18}O was preferred for dating due to its close relation to temperature and the fact that these data are available for all ice cores in the data set. The δ^{18}O signal is smoothed by diffusion in the firn, and for the low accumulation sites in the presented data set it is necessary to correct for the effect of smoothing by diffusion (Johnsen et al., 2000) before the records can be used for dating. Uncertainties associated with stratigraphic ice core timescales include loss of core or data, insufficient measuring resolution, imperfect core stratigraphy and misinterpretation of annual layers when counting (Alley et al., 1997). For the time periods relevant to this study, core and data loss is insignificant, the data resolution is sufficient (~6 samples/yr for the coarsest resolved cores) and the relatively high accumulation rates make it unlikely to have full years of missing accumulation. The risk of misinterpreting layers is always present and it is higher for low accumulation areas, where correction for diffusion is necessary. The uncertainty in the recognition of annual layers is believed to be $\sim 1\%$.

The thickness of each annual layer as determined in the isotope curve is corrected for changes in density with depth in the firn using a Herron–Langway densification model (Herron and Langway Jr., 1980) and the deeper layers are corrected for flow-induced thinning using a 1-dimensional Dansgaard–Johnsen model (Dansgaard and Johnsen, 1969). Thus the δ^{18}O data are used to infer accumulation rates as well as temperatures. All accumulation rates discussed in this work are given in ice equivalent.

Our data set contains six cores with data reaching more than a few tens or hundreds of years back in time (cf. Table 1). These six long records are used to investigate the relation between δ^{18}O and accumulation on somewhat longer time scales of up to a few thousand years. These data are shown in Fig. 2.

In order to investigate the δ^{18}O-accumulation relationship in different parts of the Greenland ice sheet, the sites are divided into six groups based on their locations: Northwest (NW), Northeast (NE), Central west (CW), Central east (CE), Southwest (SW), and Southeast (SE). The boundary between the east and west groups is defined by the ice divide. Sites located on the ice divide have been sorted into the west group in the northern and central groups but into the east group in the south, because the dominating moisture transport is from the southeast in Southern Greenland and from the west in the central and northern parts of the ice sheet. In Table 1 it is stated which group each site has been sorted into. The data from Renland have been omitted in this analysis, because

Renland is a separate ice dome and thus not part of the main ice sheet.

4 Results and discussion

From Fig. 2 it is seen that the annual data show a quite noisy relationship between δ^{18}O and accumulation rate. By using averages over longer time periods, the relationship becomes clearer. As the changes we are interested in have happened over the last 1–2 decades we choose to use 10-yr mean values in the following to keep a balance between noise-level and time resolution. The spread in accumulation rate differs between the sites. For NGRIP, GRIP, Crete and Milcent the standard deviation on the accumulation rate is 15–20% while it is higher for Dye-3 and Renland (25–30%). In the case of Dye-3, layers older than ~ 350 yr are affected by complicated upstream depositional conditions (Vinther et al., 2006). This probably explains at least part of the large spread in the calculated accumulation rates as we have not corrected for upstream effects. As for Renland, the higher spread may be explained by its location on the East coast of Greenland where the weather patterns may show larger variability than on the main ice sheet. A data set consisting of average values of temperature and ice equivalent accumulation rate for each decade from 1900 to 2009 (or the part of this period covered by each of the 52 cores) is provided in the Supplement.

Figure 3 shows 10 yr averages of accumulation rate and δ^{18}O for the 51 coring sites located on the main ice sheet. It is seen that no common Greenland relationship between δ^{18}O and accumulation rate exists. This is not surprising as the shape of the ice sheet is complex and moisture reaches different parts of the ice sheet via different routes. Assuming that the relationship between δ^{18}O and accumulation rate is exponential (Johnsen et al., 1989), least squares fits to the data in the six groups give the following relationships that we have chosen to state with a factor of 0.23 in front of the exponential to ease comparison with Eq. (1)

$$A_{\mathrm{NW}} = 0.23 \exp\left(0.100\left(\delta^{18}\mathrm{O} + 33.64\right)\right) \qquad R^2 = 0.85 \tag{3}$$

$$A_{\mathrm{NE}} = 0.23 \exp\left(0.023\left(\delta^{18}\mathrm{O} + 16.75\right)\right) \qquad R^2 = 0.05 \tag{4}$$

$$A_{\mathrm{CW}} = 0.23 \exp\left(0.140\left(\delta^{18}\mathrm{O} + 35.40\right)\right) \qquad R^2 = 0.90 \tag{5}$$

$$A_{\mathrm{CE}} = 0.23 \exp\left(0.137\left(\delta^{18}\mathrm{O} + 35.21\right)\right) \qquad R^2 = 0.49 \tag{6}$$

$$A_{\mathrm{SW}} = 0.23 \exp\left(-0.060\left(\delta^{18}\mathrm{O} + 20.18\right)\right) \qquad R^2 = 0.16 \tag{7}$$

$$A_{\mathrm{SE}} = 0.23 \exp\left(0.122\left(\delta^{18}\mathrm{O} + 34.40\right)\right) \qquad R^2 = 0.43 \tag{8}$$

Dye-3 data older than 300 yr were omitted when calculating the least square fit to the data from the SE area, because upstream effects cause artifacts in the layer thicknesses for older data.

The R^2 values differ considerably from group to group. This is to some extent explained by the varying number of data points in the groups (from 10 points in the NE group to more than 600 in the

CW group). The groups with many data points (containing long individual data series) are also the groups with the highest R^2 values. The two groups from Southern Greenland differ from the other groups in having a large fraction of very short cores which for the main part span the period from the middle of the 1960's to the middle of the 1970's. These cause a larger scatter in the data and thus a lower R^2 value.

In the southern part of the ice sheet, a positive correlation between δ^{18}O and accumulation rate is found east of the ice divide, while a negative correlation is seen to the west (Fig. 3: magenta and cyan, respectively). The dominating moisture transport across the ice divide is from the east, and the negative correlation west of the divide can be explained by the Foehn effect (warm, dry air). In the northern part of the ice sheet, all sites are located either on the divide or just east of it (black and green in Fig. 3). The sites east of the divide have lower accumulation than the sites that are located on the divide, but since there are only few data points in the NE group the relationship in Eq. (4) is not well defined. In Central Greenland no trend across the ice divide is seen (red and blue in Fig. 3). However, all sites in the CE group are located very close to the ice divide, so a Foehn effect east of the divide in Central Greenland can not be ruled out. However, the few data points from the northeast indicate a quick drop in accumulation rate on the lee side of the divide, and the same holds true for the southeastern sites close to the divide. Furthermore, the CW data set contains several long individual data series, while the data series from the CE region is generally of intermediate length. This inhomogeneity could also mask a drop in accumulation rate across the divide. If there is a lack of an effect across the divide in Central Greenland this might be explained by the fact that the area around the divide is broader and flatter and thus the orographic barrier is not as well defined as in South Greenland.

Table 2 shows the sensitivities of accumulation rate to changes in δ^{18}O and to changes in temperature assuming the relationship from Eq. (2). Two previously published values for GRIP are also shown for comparison. The values found in this study for the central part of the ice sheet agree with the value given by Dansgaard et al. (1993). Furthermore, the sensitivity seems to be lower in the north compared to the central and southern parts of the ice sheet.

Out of the 52 sites in the data set, only five records contain information on the recent warming over the last couple of decades. The δ^{18}O record from ACT10A only goes back to 1994 AD, and since we have no information on previous conditions at this site, the record can not be used to draw conclusions about recent changes. Figure 4 shows the mean values of accumulation rate and δ^{18}O for each decade since 1900 AD for the remaining four sites. No conclusive statement can be made about recent changes in accumulation rate from these data. However, the δ^{18}O values for the most recent decade at the NGRIP, B26 and NEEM sites are increasing indicating increasing temperatures. For NEEM and B26 the decade after 2000 AD has the "warmest" mean δ^{18}O value of the whole data periods of 270 yr and 110 yr, respectively, while the NGRIP record of 1820 yr shows only four decades with higher mean δ^{18}O value than the 2000–2009 decade.

5 Summary and conclusions

A data set consisting of decadal means of δ^{18}O and accumulation rates derived from annual layers determined in the δ^{18}O curves from 52 ice core sites in Greenland was presented. Out of these records, six span longer time periods than a few hundred years, and four can be used to study the period of recent warming from the 1990's and onwards. From the long records it is clear that annual accumulation and δ^{18}O data are quite noisy. However, as the averaging period is increased, the relationship between accumulation and δ^{18}O becomes clearer.

Using 10 yr averages of δ^{18}O and accumulation rates for the 51 sites located on the main ice sheet, we found that no common δ^{18}O-accumulation relation exists for Greenland. Considering the complicated shape of the ice sheet and local differences in moisture transport this is not surprising. However, the data fall into six groups according to location. In Southern Greenland a significant Foehn effect is seen across the ice divide resulting in a negative correlation between δ^{18}O and accumulation on the lee (west) side of the ice divide. In Northern Greenland we only have few data on the lee side (east) of the ice divide, but the data that do exist show a drop in accumulation rate across the divide and also indicate a significant change in the δ^{18}O-accumulation relationship. In Central Greenland, however, the data do not indicate a significant effect of the ice divide. This may be explained by the divide in Southern Greenland being more pronounced with steeper slopes on either side thus constituting a sharper barrier. The sensitivity of accumulation rate to changes in temperature seems to be smaller in Northern Greenland than in the central and southern areas.

Three of the four records that contain recent data indicate increasing temperature for the decade after 2000 AD. For NEEM and B26 the decade 2000–2009 has the warmest δ^{18}O value of the records of 270 yr, and 110 yr, respectively. In the 1820 yr long record from NGRIP only four decades have warmer δ^{18}O values than 2000–2009. At Camp Century no increase in accumulation rate or δ^{18}O can be seen, and the record from ACT10A is too short to draw any conclusions from. Thus, no conclusive statement can be made about accumulation rate from these ice core data, but they indicate an increase in temperature after 2000 AD. However, data is sparse and concentrated along the ice divide in Northern Greenland. New data series spanning at least the last 100 yr are needed from more sites in order to determine how recent temperature changes affect the accumulation rates on the Greenland ice sheet.

From this study of ice core data we conclude that the relationship between δ^{18}O and accumulation rate in Greenland show geographical differences. The effect of the ice divide is strong in Southern Greenland, and the sensitivity of accumulation rate to changes in temperature seems to be smaller in the northern part of the ice sheet than in the central and southern parts. There is too little data to draw any major conclusions about recent changes in accumulation rates.

Acknowledgements. We acknowledge the ice2sea project, funded by the European Commission's 7th Framework Programme through grant number 226375, ice2sea manuscript number 103.

References

Abdalati, W. and Steffen, K.: Greenland ice sheet melt extent: 1979–1999, J. Geophys. Res., 106, 33983–33988, 2001.

Ablain, M., Cazenave, A., Valladeau, G., and Guinehut, S.: A new assessment of the error budget of global mean sea level rate estimated by satellite altimetry over 1993–2008, Ocean Sci., 5, 193–201, doi:10.5194/os-5-193-2009, 2009.

Alley, R. B., Shuman, C. A., Meese, D. A., Gow, A. J., Taylor, K. C., Cuffey, K. M., Fitzpatrick, J. J., Grootes, P. M., Zielinski, G. A., Ram, M., Spinelli, G., Elder, B.: Visual-stratigraphic dating of the GISP2 ice core: Basis, reproducibility, and application, J. Geophys. Res., 102(C12), 26,36726,381, doi:10.1029/96JC03837, 1997.

AMAP, 2011: Snow, Water, Ice and Permafrost in the Arctic (SWIPA): climate change and the cryosphere, Arctic monitoring and assessment programme (AMAP), Oslo, Norway, 538 pp., 2011.

Box, J. E.: Survey of Greenland instrumental temperature records: 1873–2001, Int. J. Climatol., 22, 1829–1847, doi:10.1002/joc.852, 2002.

Box, J. E., Bromwich, D. H., Veenhuis, B. A., Bai, L.-S., Stroeve, J. C., Rogers, J. C., Steffen, K., Haran, T., and Wang, S.-H.: Greenland ice sheet surface mass balance variability (1988–2004) from calibrated Polar MM5 output, J. Climate, 19, 2783–2800, 2006.

Box, J. E., Yang, L., Bromwich, D. H., and Bai, L.-S.: Greenland ice sheet surface air temperature variability: 1840–2007, J. Climate, 22, 4029–4049, 2009.

Dahl-Jensen, D., Johnsen, S. J., Hammer, C. U., and Jouzel, J.: Past accumulation rates derived from observed annual layers in the GRIP ice core from Summit, Central Greenland, in: NATO ASI Series, Vol. 1, 12, Ice in the Climate System, edited by: Peltier, W. R., Springer, Berlin, 517–532, 1993.

Dansgaard, W.: The abundance of O^{18} in atmospheric water and water vapour, Tellus 5, 461–469, 1953.

Dansgaard, W.: Stable isotopes in precipitation, Tellus 16, 436–468, 1964.

Dansgaard, W. and Johnsen, S. J.: A flow model and a time scale for the ice core from Camp Century, Greenland, J. Glaciol., 8, 215–223, 1969.

Dansgaard, W., Johnsen, S. J., Clausen, H. B., Dahl-Jensen, D., Gundestrup, N. S., Hammer, C. U., Hvidberg, C. S., Steffensen, J. P., Sveinbjörnsdottir, A. E., Jouzel, J., and Bond, G.: Evidence for general instability of past climate from a 250-kyr ice-core record, Nature, 364, 218–220, 1993.

Hammer, C. U.: Acidity of polar ice cores in relation to absolute dating, past volcanism, and radio-echos, J. Glaciol., 25, 359–372, 1980.

Hammer, C. U., Clausen, H. B., Dansgaard, W., Gundestrup, N., Johnsen, S. J., and Reeh, N.: Dating of Greenland ice cores by flow models, isotopes, volcanic debris, and continental dust, J. Glaciol., 20, 3–26, 1978.

Herron, M. M. and Langway Jr., C. C.: Firn densification: an imperial model, J. Glaciol., 25, 373–385, 1980.

IPCC, Climate Change 2007: The Physical Science Basis, Contribution of Working Group I to the Fourth Assessment Report of the Intergovernmental Panel on Climate Change, edited by: Solomon, S., Qin, D., Manning, M., Chen, Z., Marquis, M., Averyt, K. B., Tignor, M., and Miller, H. L., Cambridge University Press, Cambridge, United Kingdom and New York, NY, USA, 2007.

Johnsen, S. J., Dansgaard, W. and White, J. W. C.: The origin of arctic precipitation under present and glacial conditions, Tellus B, 41, 452–468, 1989.

Johnsen, S. J., Dahl-Jensen, D., Dansgaard, W., and Gundestrup, N.: Greenland palaeotemperatures derived from GRIP bore hole temperature and ice core isotope profiles, Tellus B, 47, 624–629, 1995.

Johnsen, S. J., Clausen, H. B., Cuffey, K. M., Hoffmann, G., Schwander, J., and Creyts, T.: Diffusion of stable isotopes in polar firn and ice: The isotope effect in firn diffusion, in: Physics of Ice Core Records, edited by: Hondoh, T., Hokkaido University Press, Sapporo, 121–140, 2000.

Legrand, M. and Mayewski, P. (1997): Glaciochemistry of polar ice cores: A review, Rev. Geophys., 35(3), 219243, doi:10.1029/96RG03527, 1997.

Vinther, B. M., Clausen, H. B., Johnsen, S. J., Rasmussen, S. O., Andersen, K. K., Buchardt, S. L., Dahl-Jensen, D., Seierstad, I. K., Siggaard-Andersen, M.-L., Steffensen, J. P., Svensson, A. M., Olsen, J., and Heinemeier, J.: A synchronized dating of three Greenland ice cores throughout the Holocene, J. Geophys. Res., 111, D13102, doi:10.1029/2005JD006921, 2006.

Table 1. Greenland ice cores dated by annual layer counting in the δ^{18}O record. Annually resolved δ^{18}O data from all sites are from the Centre for Ice and Climate database.

Ice core	Latitude	Longitude	Period covered by data	Group
ACT10A	65.69	−41.48	1994–2009	SE
B26*	77.25	−49.22	1900–2009	NW
Camp Century*	77.17	−61.10	1762–2009	NW
Crete*	71.12	−37.32	554–1973	CW
Dye-2*	66.48	−46.33	1743–1973	SW
Dye-3*	65.18	−43.83	−3816–1979	SE
Dye-3 1975 (D-2)	65.16	−43.94	1965–1974	SE
Dye-3 1975 (D-3)	65.16	−43.92	1965–1974	SE
Dye-3 1975 (D-4)	65.17	−43.90	1966–1974	SE
Dye-3 1975 (D-5)	65.17	−43.88	1965–1974	SE
Dye-3 1975 (D-6)	65.18	−43.87	1966–1974	SE
Dye-3 1980 Swiss core	65.20	−43.81	1834–1979	SE
Dye-3 1981 13B	65.09	−44.24	1965–1980	SE
Dye-3 1981 SDV	65.02	−44.65	1964–1980	SW
Dye-3 1982 7B	65.14	−44.02	1967–1979	SE
Dye-3 1983 4B	65.17	−43.93	1692–1981	SE
Dye-3 1984 5B	65.16	−43.88	1956–1982	SE
Dye-3 1984 9B	65.12	−44.09	1955–1983	SE
Dye-3 1984 11B	65.11	−44.16	1955–1983	SE
Dye-3 1984 15B	65.08	−44.30	1954–1983	SE
Dye-3 1984 16C	65.05	−44.33	1955–1983	SE
Dye-3 1984 18C	65.03	−44.39	1777–1983	SE
GRIP*	72.57	−37.62	−1846–1989	CW
Milcent 1973	70.30	−45.00	1177–1966	CW
NEEM*	77.45	−51.08	1737–2009	NW
NGRIP*	75.10	−42.32	187–2007	NW
North Central*	74.62	−39.60	1910–1976	NE
North Site 1972	75.77	−42.45	1925–1971	NE
Renland*	71.31	−26.72	931–1986	–
Saddle North 1975 (SN)	66.17	−43.78	1967–1974	SE
Saddle North 1975 Satelite 1 (SNS-1)	66.47	−44.83	1961–1974	SW
Saddle South 1975 (SAS)	65.68	−44.33	1966–1974	SE
Saddle South 1975 satelite 1 (SDS-1)	65.70	−44.76	1964–1974	SW
Saddle South 1975 satelite 2 (SDS-2)	65.53	−44.12	1966–1974	SE
Saddle South 1975 satelite 3 (SDS-3)	65.83	−44.12	1966–1974	SE
Site A (Crete region) 1985	70.63	−35.82	1623–1984	CE
Site A-1 1975 (Dye-3 region)	67.50	−42.20	1965–1974	SE
Site A-1 1975 Satelite 1 (A-1-S-1)	67.03	−41.85	1967–1974	SE
Site A-1 1975 Satelite 2 (A-1-S-2)	67.85	−43.12	1961–1974	SW
Site B (Crete region) 1984	70.65	−37.48	1717–1983	CW
Site BDS 1975 (Dye-3 region)	64.50	−44.33	1965–1974	SE
Site C (Crete region) 1984	70.68	−38.78	1943–1983	CW
Site D (Crete region) 1984	70.63	−39.62	1767–1982	CW
Site E (Crete region) 1985	71.77	−35.85	1722–1984	CE
Site F (Crete region) 1985	71.50	−35.88	1925–1982	CE
Site G (Crete region) 1985	71.15	−35.83	1778–1984	CE
Site H (Crete region) 1985	70.87	−35.83	1933–1983	CE
South Dome 1975	63.53	−44.58	1869–1974	SE
South Dome 1975 Satelite 1 (DS-1)	63.60	−44.25	1968–1974	SE
South Dome 1975 Satelite 2 (DS-2)	63.55	−44.93	1962–1974	SW
South Dome 1975 Satelite 3 (DS-3)	63.70	−44.58	1964–1974	SW
SUMMIT 1974	72.28	−37.98	1904–1971	CW

Table 2. The sensitivity of accumulation rate A to changes in δ^{18}O and temperature T. The given uncertainties are derived from the uncertainty in the least squares estimation of the parameters in Eqs. 3–8 and do not represent the total uncertainty which is larger.

Group	$\frac{1}{A}\frac{\partial A}{\partial \delta}$ (%‰$^{-1}$)	$\frac{1}{A}\frac{\partial A}{\partial T}$ (%K^{-1})
NW	10.0±0.3	6.7±0.2
NE	2.3±4.2	1.5±2.8
CW	14.0±0.2	9.4±0.1
CE	13.7±1.5	9.2±1.0
SW	−6.0±2.7	−4.0±1.8
SE	12.2±1.2	8.2±0.8
GRIP (from Dahl-Jensen et al., 1993)	11.7	7.8
GRIP (from Dansgaard et al., 1993)	14.4	9.6

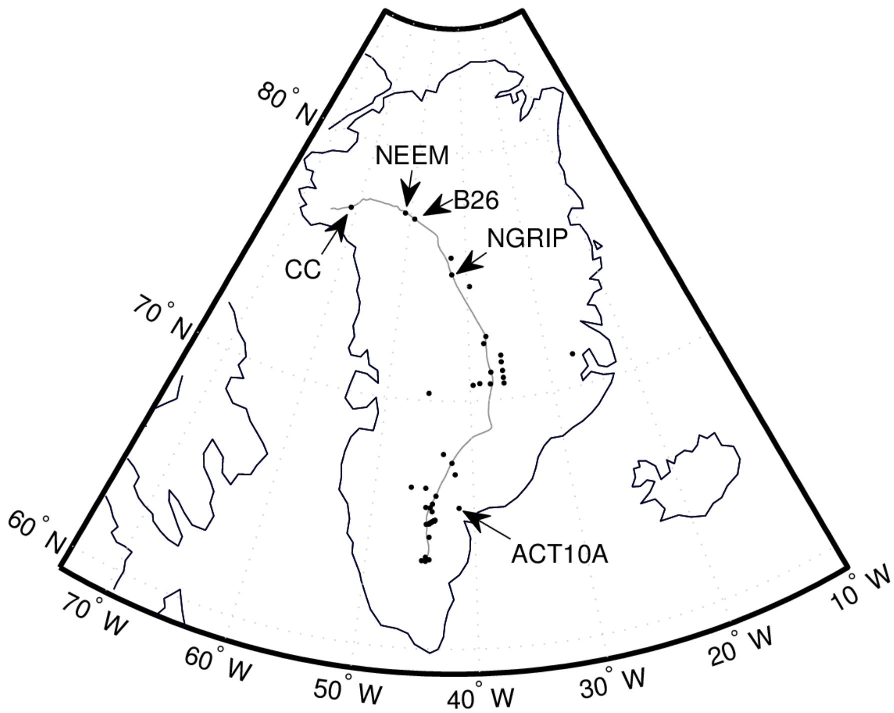

Fig. 1. The locations of the 52 ice core sites listed in Table 1. The five sites from which we have data for the most recent decade are indicated with labeled arrows.

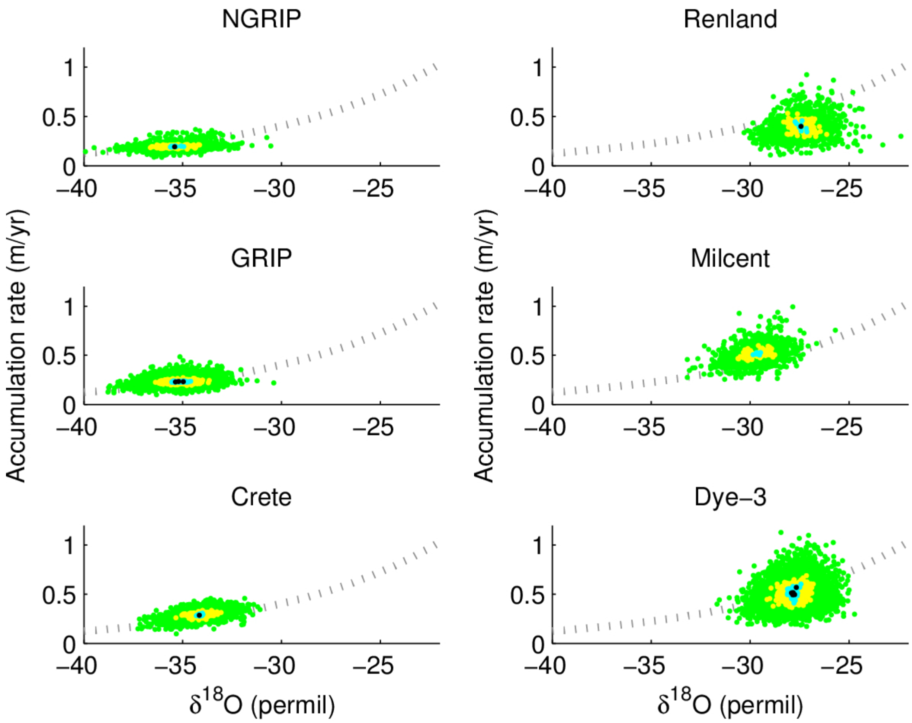

Fig. 2. Mean values of accumulation rate and δ^{18}O for the six longest records in our data set. The averaging periods are 1 yr (green), 10 yr (yellow), 100 yr (cyan), and 1000 yr (black). The dotted grey line shows the relation from Dahl-Jensen et al. (1993) (Eq. 1). See Table 1 for the time periods covered by each data series.

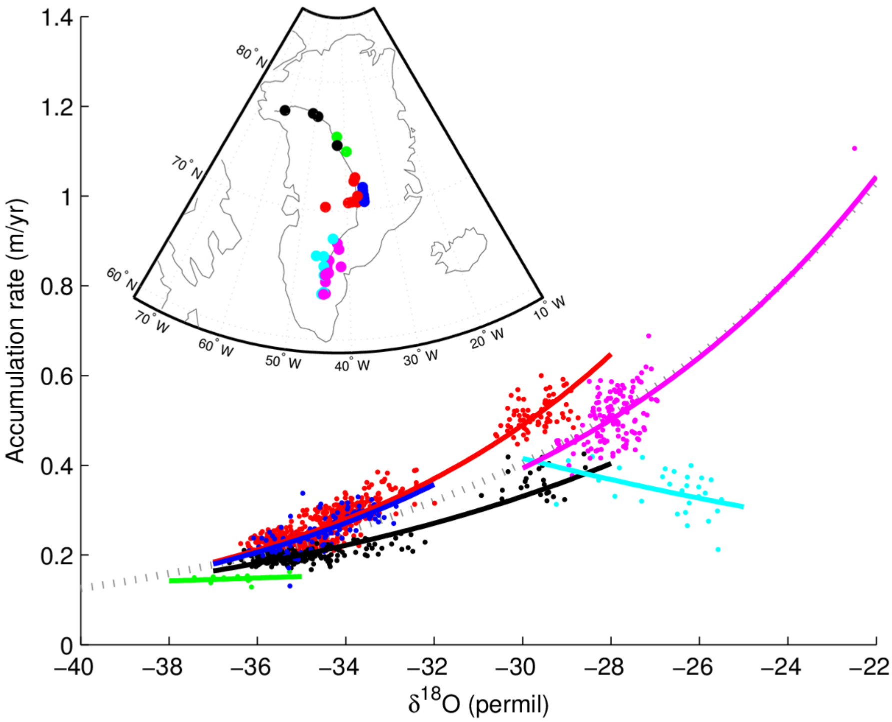

Fig. 3. 10 yr averages of ice equivalent accumulation rate and δ^{18}O from 51 sites on the Greenland ice sheet. The sites have been sorted into six groups according to location: Northwest (black), Northeast (green), Central west (red), Central east (blue), Southwest (cyan), and Southeast (magenta). The least squares exponential fits to the data for each of the groups are shown in the corresponding colour and the relation from Dahl-Jensen et al. (1993) is shown for comparison (dotted grey curve). The insert shows the locations of the 51 core sites with colours indicating the grouping of the sites. For Dye-3, data is only shown for the last 300 yr as the thickness of layers older than this are affected by upstream conditions.

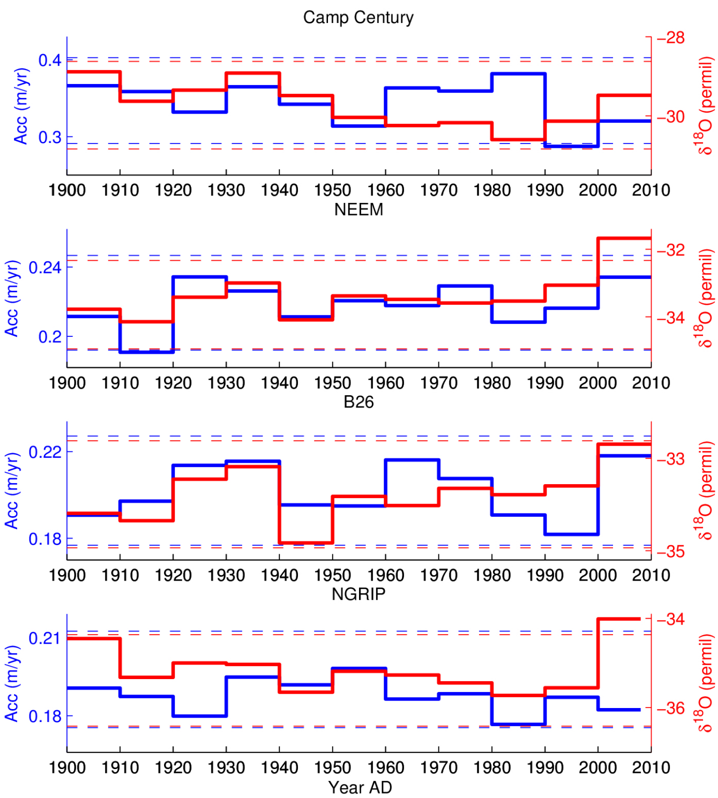

Fig. 4. Average values of accumulation rates (blue) and δ^{18}O values (red) for each decade since 1900 AD. The blue and red dashed lines indicate the mean value $\pm 2\sigma$ of accumulation rate and δ^{18}O, respectively, for the whole data period for each site. The periods of data for the four sites are: Camp Century: 1762–2009 AD, NEEM: 1737–2009 AD, B26: 1900–2009 AD, and NGRIP: 187–2007 AD.